White Rose Research Online

eprints@whiterose.ac.uk
https://eprints.whiterose.ac.uk
Universities of Leeds, Sheffield and York

Deposited via The University of Sheffield.

White Rose Research Online URL for this paper:
https://eprints.whiterose.ac.uk/id/eprint/141433/

Version: Accepted Version

Article:
Poluri, N. and De Souza, M.M. (2019) High-efficiency modes contiguous with class B/J and continuous class F^{-1} amplifiers. IEEE Microwave and Wireless Components Letters, 29 (2). pp. 137-139. ISSN: 1531-1309

https://doi.org/10.1109/LMWC.2018.2886655

© 2019 IEEE. Personal use of this material is permitted. Permission from IEEE must be obtained for all other users, including reprinting/ republishing this material for advertising or promotional purposes, creating new collective works for resale or redistribution to servers or lists, or reuse of any copyrighted components of this work in other works. Reproduced in accordance with the publisher's self-archiving policy.

Reuse
Items deposited in White Rose Research Online are protected by copyright, with all rights reserved unless indicated otherwise. They may be downloaded and/or printed for private study, or other acts as permitted by national copyright laws. The publisher or other rights holders may allow further reproduction and re-use of the full text version. This is indicated by the licence information on the White Rose Research Online record for the item.

Takedown
If you consider content in White Rose Research Online to be in breach of UK law, please notify us by emailing eprints@whiterose.ac.uk including the URL of the record and the reason for the withdrawal request.

UNIVERSITY OF LEEDS
University of Sheffield
UNIVERSITY of York

High-Efficiency Modes Contiguous with Class B/J and Continuous Class F^{-1}amplifiers

Nagaditya Poluri and Maria Merlyne De Souza, *Senior Member, IEEE*

***Abstract*— We propose a new formulation for high-efficiency modes of power amplifiers in which both the in-phase and out-of-phase components of the second harmonic of the current are varied, in addition to the second harmonic component of the voltage. A reduction of the in-phase component of the second harmonic of current allows reduction of the phase difference between the voltage and current waveforms, thereby increasing the power factor and efficiency. Our proposed waveforms offer a continuous design space between the class B/J continuum and continuous F^{-1} achieving an efficiency of up to 91% in theory, but over a wider design space than F^{-1}. These waveforms require a short at third and higher harmonic impedances which are easier to achieve at higher frequency. The fabricated amplifier using a GaN HEMT CGH40010F achieves 79.7% drain efficiency and 42.2 dBm saturated output power at 2.6 GHz, which gives a frequency weighted efficiency of 92.4% $\sqrt[4]{GHz}$ with this device.**

***Index Terms*—Class B/J/J* continuum, Continuous class F^{-1}, High efficiency, Power amplifier, GaN HEMT**

I. Introduction

THE class B/J continuum for amplifier design, first proposed by Cripps [1], utilizes the second harmonic of voltage to increase the fundamental component through the device. An increase in the magnitude of this second harmonic by a factor of α/2, where α∈[-1,1], increases the fundamental component by $\sqrt{1+\alpha^2}$. However, such an approach does not benefit the efficiency nor the output power of the amplifier because of the corresponding increase in mismatch between the phase of the fundamental components of voltage and current [2]. The only benefit of class B/J continuum is its flexibility of design space.

Shaping the drain current waveform for a high quadrature second harmonic component by generating suitably phased harmonics at the input voltage via a varactor diode is shown to reduce the phase mismatch and increase efficiency [2]. On the other hand, continuous class F^{-1} (CCF^{-1}), proposed by Kim [3], relies on load impedances to eliminate the in-phase component of the second harmonic and manipulation of the quadrature component of the second harmonic of the current in class J. The voltage waveform of continuous class F^{-1} is the same as that in class J for |α|=1 but with fundamental and second harmonic components phase shifted by π/4 and π/2 respectively. This shift reduces the phase mismatch from π/4 in class J to 0 in class F^{-1}, thereby increasing the power factor. As a result, the drain efficiency of class F^{-1} is 91% as opposed to 78.5% in class J with a short at third and higher harmonics. These classes represent two extremities, of manipulating the second harmonic of the current. We propose a new contiguous set of current waveforms between these classes whereby the in-phase component of the second harmonic of the current in class J is partially removed to achieve higher efficiency than class J.

II. Formulation

The drain current in a class B/J continuum is [1]

$$I_{DS(J)}(\theta) = I_m/\pi + \{I_m/2\}\cos(\theta) + \{(2I_m)/3\pi\}\cos(2\theta) + \cdots \quad (1)$$

Where, I_m is the maximum current of the device. The fundamental and second harmonic load impedances result in removal of the second harmonic component ($i_2(\theta)$) from $I_{DS(J)}(\theta)$ [3]. The resulting drain current of the device ($I_{ds}(\theta)$), is given as

$$I_{DS}(\theta) = \begin{cases} I_{DS(J)}(\theta) - i_2(\theta) & \left(2p-\frac{1}{2}\right)\pi < \theta < \left(2p+\frac{1}{2}\right)\pi \\ 0 & otherwise \end{cases} \quad (2)$$

Where, p is an integer. We express $i_2(\theta)$ as in (3), wherein, the in-phase component of the second harmonic of the current in class J is partially removed by a factor (k).

$$i_2(\theta) = k\{(2I_m)/3\pi\}\{2\cos(2\theta)\} - C_Q\sin(2\theta);\ 0 \le k \le 1 \quad (3)$$

Where, C_Q is an arbitrary real number. The minimum of $|C_Q|$ is zero and the maximum it can attain is such that the peak current of $I_{DS}(\theta)$ is I_m. k = C_Q = 0, in class B/J continuum [1] whereas k=1 in CCF^{-1} [3]. $I_{DS}(\theta)$ can be approximated as

$$I_{DS}(\theta) \approx I_m/\pi + A_{i1}\cos(\theta) + B_{i1}\sin(\theta) + A_{i2}\cos(2\theta) + B_{i2}\sin(2\theta) + A_{i3}\cos(3\theta) + B_{i3}\sin(3\theta) \quad (4)$$

Where,

$$A_{i1} = I_m\left[\frac{1}{2} - \frac{8k}{9\pi^2}\right];\ A_{i2} = \frac{2I_m}{3\pi}(1-k);\ A_{i3} = -\frac{8kI_m}{5\pi^2} \quad (5)$$

$$B_{i1} = 8\beta A_{i1}/(3\pi);\ B_{i2} = C_Q = \beta A_{i1};\ B_{i3} = 8\beta A_{i1}/(5\pi) \quad (6)$$

Where, we define β as C_Q/A_{i1}. The phases of the fundamental (θ_1) and second harmonic (θ_2) components of the current are

$$\theta_1 = \tan^{-1}(8\beta/3\pi);\ \theta_2 = \tan^{-1}(\beta\{3\pi/4 - 4k/(3\pi)\}/(1-k)) \quad (7)$$

We propose drain voltage waveforms with a phase of ±π/2 at the second harmonic frequency, so that the load at the second harmonic is purely reactive, and remains above the knee voltage (V_k) for all values of k in the following equation (8) as:

$$V_{DS} = V_k + (V_{DC} - V_k)\{1 - \cos(\theta - \theta_2/2) - \alpha\sin(\theta - \theta_2/2) + \alpha\sin(2\theta - \theta_2)/2\} \quad (8)$$

This voltage waveform is obtained by shifting the fundamental and second harmonic components of the voltage waveform of

Manuscript received on June 30, 2018. Revised on November 5, 2018. Revised on December 11, 2018. The authors are with the EEE department, University of Sheffield, Sheffield, S37HQ, UK (e-mail: npoluri1@sheffield.ac.uk and m.desouza@sheffield.ac.uk). MMS acknowledges support from ENIAC- JU project PARSIMO under grant contract – 270687

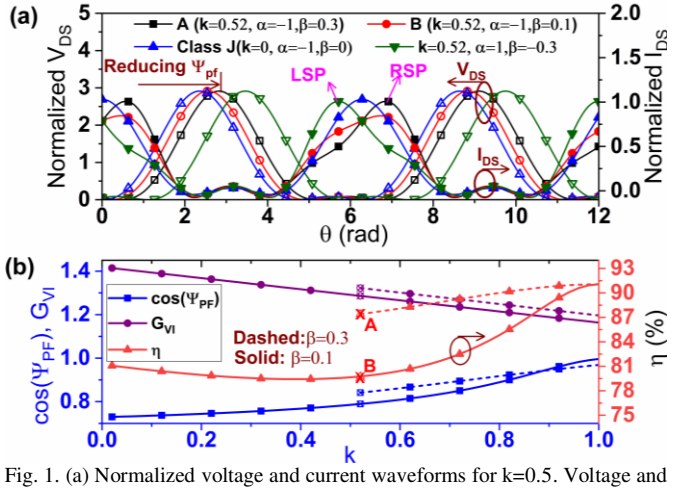

Fig. 1. (a) Normalized voltage and current waveforms for k=0.5. Voltage and current waveforms obtained by setting V_{DC}=1, I_m=1, and V_k=0. LSP and RSP denote the left-side peaking and right-side peaking respectively. (b) Power factor ($\cos(\Psi_{pf})$), Current-Voltage gain (G_{VI}), and efficiency as k increases from 0 to 1 for α=-1, and β=0.3 and 0.1,

class B/J by $\theta_2/2$ and θ_2 respectively, giving an overall phase difference between the fundamental components of the current and voltage waveforms Ψ_{pf} as:

$$\Psi_{pf} = \Psi_{pf(J)} - \theta_1 + \theta_2/2;\ \Psi_{pf(J)} = \tan^{-1}(\alpha) \quad (9)$$

Where, $\Psi_{pf(J)}$ is the phase difference between the current and voltage waveform in class J. As k is increased from 0 to 1, from (7), θ_2 increases from 0 to $\pi/2$ if β is positive or 0 to $-\pi/2$ if β is negative. Hence by choosing α and β with opposite signs, from (9), it can be observed that θ_2 negates the effect of α in $\Psi_{pf(J)}$. The voltage and current waveforms in class J and our proposed class for k=0.52 are plotted in Fig. 1 (a), to demonstrate the reduction in phase difference. β >0 and β <0 result in a peaking of current to the right and left, respectively.

The output power (P_{out}) and efficiency (η) can be expressed in terms of the output power ($P_{out|B}$) and efficiency (η_B) of class B as

$$P_{out}/P_{out|B} = \eta/\eta_B = G_{VI}\cos(\Psi_{pf}) \quad (10)$$

Where, G_{VI} is defined as the gain in the product of the current and voltage over class B, calculated as

$$G_{VI} = (1 - 16k/(9\pi^2))\sqrt{\{1+\alpha^2\}\{1+(64\beta^2)/(9\pi^2)\}} \quad (11)$$

The power factor ($\cos(\Psi_{pf})$), G_{VI} and efficiency with k are plotted in Fig. 1 (b). The power factor increases due to a reduction of Ψ_{pf} as k increases, whereas, G_{VI} reduces with k due to the reduction of A_{i1} with k. The increase in power factor compensates for the reduction in G_{VI} resulting in an efficiency and output power higher than in class B/J; waveforms 'A' and 'B' marked in Fig. 1 (a) achieve 2% and 9% higher efficiency than class J. Not only the efficiency, but also the output power of the proposed mode is higher than class J, in proportion to the efficiency as revealed by (11). On the other hand, adjustment of the loadline to increase efficiency results in a tradeoff with output power, which is not the case in this work. In the extreme case of k=1 and $|\alpha|$=1, which corresponds to CCF^{-1}, $|\theta_2|$ is $\pi/2$, resulting in the minimum phase difference between the fundamental components of the voltage and current, resulting in an efficiency of 91% [3]. θ_1, θ_2 and G_{VI} increase with

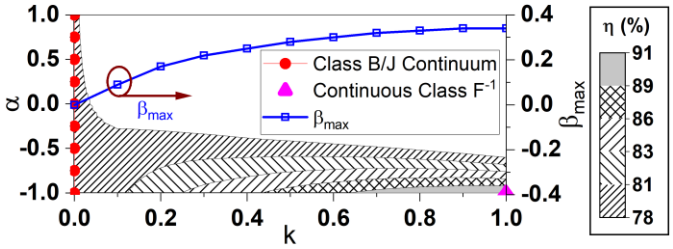

Fig. 2. The maximum allowable value of β vs k. The contours of efficiency with α and k for β= β_{max} calculated from (11). V_{DC}=1V, I_m=1A, and V_k=0V were used for this simulation. Shaded regions demonstrate design flexibility in comparison to continuous class F^{-1} and class B/J.

increase in β as seen from (8) and (12), resulting in higher efficiencies in Fig. 1 (b). The increase in θ_1 results in a lower power factor for β=0.3 than β=0.1 as k approaches 1.

The maximum allowable value of β (β_{max}) for a given k and the contours of efficiency (η) with α and k when β= β_{max} are plotted in Fig. 2. As k increases from 0 to 1, the in-phase components (A_{i1} and A_{i2}) decrease and hence β_{max} increases. The efficiency can be maintained within 2% over a range of waveforms defined by k, α, and β. The continuum of waveforms for k>0, except for CCF^{-1}, have not been previously described. Reducing $|\alpha|$ while maintaining constant k and β, reduces efficiency and output power because the magnitude of the fundamental component of the voltage decreases. Hence, the minimum $|\alpha|$ required to achieve η>78% increases with increase in k due to the reduction of the fundamental component of current. Because these waveforms are contiguous with class J and CCF^{-1} with both these classes at extremities, the linearity of these modes lies in between these two classes.

III. Implementation and Results

A 10 W GaN HEMT from Cree, CGH40010F, is chosen for this study. The device is biased in deep class AB mode (V_{dsq}=28 V, I_{dsq}=150 mA) and (α, β, k) = (-0.6,0.3,0.7) are chosen for this implementation. The optimal loadline resistance (R_{opt}) is found to be 38.1 Ω. The impedances at fundamental ($Z_{1,int}$) and second harmonic ($Z_{2,int}$) frequencies, required to maintain the waveforms are calculated from (4) and (8) , are

$$Z_{1,int} = \frac{R_{opt}\sqrt{1+\alpha^2}e^{-i\Psi_{pf}}}{\left([1-16k/(9\pi^2)]\sqrt{1+(8\beta/3\pi)^2}\right)} \quad (12)$$

$$Z_{2,int} = \frac{i\alpha R_{opt}}{\sqrt{\{8(1-k)/(3\pi)\}^2 + \{2\beta - (32\beta k)/(9\pi^2)\}^2}} \quad (13)$$

The impedances at the extrinsic plane at 2.6 GHz are calculated from $Z_{1,int}$ and $Z_{2,int}$. To account for non-idealities of the device, the corresponding extrinsic impedances at fundamental ($Z_{1,ext}$) and second harmonic ($Z_{2,ext}$) frequencies are adjusted from load pull simulations using the vendor model. These impedances are plotted in Fig. 3(a). The ratios $|\Im m(Z_{1,int})/\Im m(Z_{2,int})|$ and $|\Im m(1/Z_{1,int})/\Im m(1/Z_{2,int})|$ are 1.15π and 2π, neither equal to 3π/8 as in class B/J continuum and continuous class F^{-1}; showing a paradigm shift from the conventional continuum. The output and input matching networks are realized on a 0.762 mm thick R4350B substrate using three stub and stepped impedance topologies, respectively. The measured impedances are plotted in Fig. 3(a)

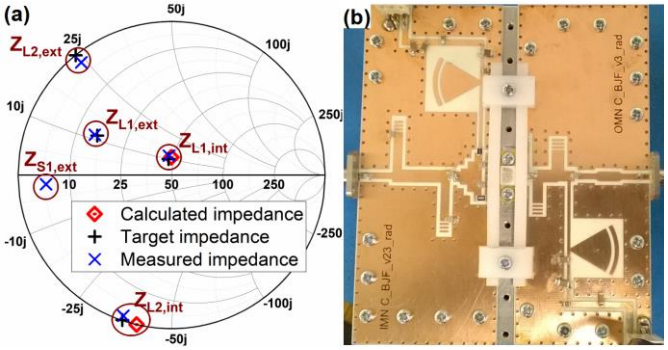

Fig. 3. (a) Calculated, target, and measured impedances at $Z_{L1,int}$ and $Z_{L2,int}$ of the output matching network. Target and realized impedances at $Z_{L1,ext}$ and $Z_{L2,ext}$ at the extrinsic plane. The measured source impedance ($Z_{S1,ext}$) at 2.6GHz of the input matching network. (b) Photograph of the designed amplifier

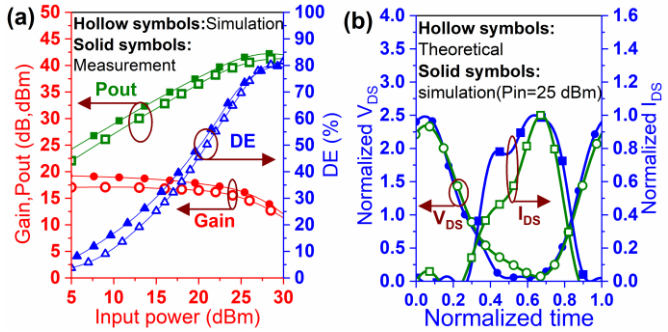

Fig. 4. (a) The measured and simulated gain, output power (P_{out}), and drain efficiency (DE) of the designed amplifier. (b) The intrinsic voltage and current waveforms from the simulation and the theoretical waveforms. The voltage and current are normalized to V_{DC} and I_m respectively. V_{DC}=28 V, V_k=2 V, and R_{opt}=38.1 Ω were used for the calculation of I_{DS} and V_{DS}.

and closely match with the target impedances. The photograph of the designed amplifier is shown in Fig. 3(b).

The gain, output power, and DE of the fabricated amplifier in Fig. 4(a), demonstrates 79.7% DE and 42.2 dBm output power at 2.6 GHz. The intrinsic voltage and current waveforms obtained from harmonic balance simulation and from theoretical calculation are plotted in Fig. 4(b). The peaking of current to the right and the increase of the maximum of normalized voltage $V_{DS,}$ in excess of a factor of 2V, reveal the manipulation of the second harmonic of both the voltage and current waveforms, conforming with theory. The response of the amplifier with frequency is plotted in Fig. 5, revealing a near flat output power, PAE>58%, and DE>65% over a 600 MHz 24% fractional bandwidth, despite being designed narrowband at 2.6 GHz. Its performance is compared with other state-of-the-art amplifiers using the same device in Table I. The designed amplifier achieves higher or comparable frequency weighted efficiency (FE) and delivers higher output power over the bandwidth than other amplifiers. Additionally, the design methodology presented here requires tuning second harmonic only whereas the other works in Table I require impedances up to 3rd harmonic whilst designing the matching network.

IV. Conclusion

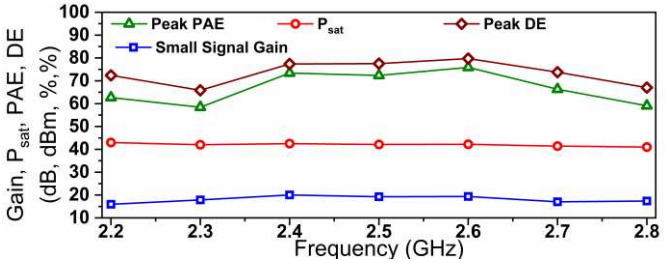

Fig. 5. Measured peak PAE, peak DE, Maximum Output power, and Gain of the designed amplifier with frequency over 3dB bandwidth.

TABLE I
COMPARISON OF THE DESIGNED AMPLIFIER WITH THE STATE-OF-THE-ART AMPLIFIERS USING CGH40010F REPORTED IN THE LITERATURE.

Ref.	Mode	No. of harm. tuned	Bandwidth (GHz, %)	Output power (dBm)	DE (AE) %,(%)	FE
[4]	CCF	3	0.55 - 1.1, 66.7	39.3-41.2	65-80 (74)	70.5
[5]	CCF/F-1	3	0.4-2.3, 140.7	39-42	62.3-80.5 (71)	76.5
[6]	CCF	3	1.45-2.45, 51.3	40.4-42.3	70-81 (75.9)	89.7
[7]	SCIM	3	2.4-3.9, 47.6	39.63-41.4	62-75 (68.1)	90.7
[8]	SCM	3	1.6-2.8, 54.6	40-42.5	67.5-81.9 (76.4)	92.5
T.W.	BJF-1	2	2.2-2.8, 24.0	41-43	65.9-79.7 (73.4)	92.4

AE = Average Efficiency, FE=AE*$\sqrt[4]{Center\ Freq.(in\ GHz)}$, HT = harmonic tuned, SCM = series of continuous modes, SCIM=Series of inverse continuous modes, CCF/F^{-1} = Continuous class F/F^{-1}, T.W.= This Work

A new theoretical formulation for the current and voltage waveforms achieving efficiency ranging from that of class B to class F^{-1} is proposed in this letter. Assisted by second harmonic manipulation, the mismatch in the phases of fundamental components of voltage and current of these waveforms is lower than in class J. An amplifier designed based on the proposed waveforms achieves 79.7% DE and 42.2 dBm output power at 2.6 GHz. A major implication of the proposed continuum is a wide design space available to designers with simultaneous high efficiency and output power in comparison to continuous class F^{-1} or class BJ, thus easing amplifier design.

References

[1] S. C. Cripps, P. J. Tasker, A. L. Clarke, J. Lees, and J. Benedikt, "On the continuity of high efficiency modes in linear RF power amplifiers," *IEEE Microw. Wirel. Components Lett.*, vol. 19, no. 10, pp. 665–667, 2009.

[2] S. C. Cripps, "RF Power Amplifiers for Wireless Communications," 2nd ed., Boston, MA: Artech, 2006.

[3] J. H. J. Kim *et al.*, "Analysis of High-Efficiency Power Amplifier Using Second Harmonic Manipulation : Inverse Class-F / J Amplifiers," *IEEE Trans. Microw. Theory Tech.*, vol. 59, no. 8, pp. 2024–2036, 2011.

[4] V. Carrubba, J. Lees, J. Benedikt, P. J. Tasker, and S. C. Cripps, "A Novel Highly Efficient Broadband Continuous Class-F RFPA Delivering 74 % Average Efficiency for an Octave Bandwidth," in *IEEE MTT-S International Microwave Symposium Digest*, 2011, vol. 2, no. 1, pp. 1–4.

[5] Q.-H. Tang, Y.-H. Li, and W.-G. Li, "Over Second Octave Power Amplifier Design Based on Resistive–Resistive Series of Continuous Class-F/F −1 Modes," *IEEE Microw. Wirel. Components Lett.*, vol. 27, no. 5, pp. 494–496, May 2017.

[6] N. Tuffy, L. Guan, A. Zhu, and T. J. Brazil, "A simplified broadband design methodology for linearized high-efficiency continuous class-F power amplifiers," *IEEE Trans. Microw. Theory Tech.*, vol. 60, no. 6 PART 2, pp. 1952–1963, 2012.

[7] W. Shi, S. He, and Q. Li, "A Series of Inverse Continuous Modes for Designing Broadband Power Amplifiers," *IEEE Microw. Wirel. Components Lett.*, vol. 26, no. 7, pp. 525–527, 2016.

[8] J. Chen, S. He, F. You, R. Tong, and R. Peng, "Design of Broadband High-Efficiency Power Amplifiers Based on a Series of Continuous Modes," *IEEE Microw. Wirel. Components Lett.*, vol. 24, no. 9, pp. 631–633, Sep. 2014.